NASA TECHNICAL MEMORANDUM

NASA TM X-3525

NASA TM X-3525

NEUTRON MONITORING AND ELECTRODE CALORIMETRY EXPERIMENTS IN THE HIP-1 HOT ION PLASMA

John J. Reinmann and Robert W. Layman

Lewis Research Center

Cleveland, Ohio 44135

NATIONAL AERONAUTICS AND SPACE ADMINISTRATION • WASHINGTON, D. C. • MAY 1977

1. Report No. NASA TM X-3525	2. Government Accession No.	3. Recipient's Catalog No.
4. Title and Subtitle NEUTRON MONITORING AND ELECTRODE CALORIMETRY EXPERIMENTS IN THE HIP-1 HOT ION PLASMA		5. Report Date May 1977 6. Performing Organization Code
7. Author(s) John J. Reinmann, Lewis Research Center; and Robert W. Layman, Dartmouth College, Hanover, New Hampshire		8. Performing Organization Report No. E-9063
9. Performing Organization Name and Address Lewis Research Center National Aeronautics and Space Administration Cleveland, Ohio 44135		10. Work Unit No. 506-25 11. Contract or Grant No.
12. Sponsoring Agency Name and Address National Aeronautics and Space Administration Washington, D. C. 20546		13. Type of Report and Period Covered Technical Memorandum 14. Sponsoring Agency Code

15. Supplementary Notes

16. Abstract

The HIP-1 plasma was a steady-state $\vec{E}\times\vec{B}$ discharge contained in a magnetic mirror geometry. It produced hydrogen ion temperatures up to 900 eV and with deuterium gas steady-state neutron activity of about 10^6 n/sec. Results are presented for two additional diagnostic procedures on HIP-1: (1) neutron diagnostics to determine where neutrons originated within the plasma discharge chamber and (2) electrode calorimetry to measure the steady-state power absorbed by the anodes and cathodes. Results are also reported for a hot-ion plasma formed with a continuous-cathode rod, one that spans the full length of the test section, in place of the two hollow cathodes. The outboard neutron source strength increased relative to that at the midplane when (1) the cathode tips were moved farther outboard, (2) the anode diameters were increased, and (3) one of the anodes was removed. The distribution of neutron sources within the plasma discharge chamber was insensitive to the division of current between the two cathodes. For the continuous cathode, increasing the discharge current increased the midplane neutron source strength relative to the outboard source strength. Each cathode absorbed from 12 to 15 percent of the input power regardless of the division of current between the two cathodes. The anodes absorbed from 20 to 40 percent of the input power. The division of power absorption between the two anodes varied with plasma operating conditions and electrode placement.

17. Key Words (Suggested by Author(s))
Plasma heating; Fusion-like plasma; Hot ion plasma; $\vec{E}\times\vec{B}$ plasma; Neutron diagnostics of plasmas; Plasma energy balance; Electrode calorimetry of $\vec{E}\times\vec{B}$ plasmas

18. Distribution Statement
Unclassified - unlimited
STAR category 75

19. Security Classif. (of this report)	20. Security Classif. (of this page)	21. No. of Pages	22. Price*
Unclassified	Unclassified	27	A03

* For sale by the National Technical Information Service, Springfield, Virginia 22161

NEUTRON MONITORING AND ELECTRODE CALORIMETRY EXPERIMENTS IN THE HIP-1 HOT ION PLASMA*

by John J. Reinmann and Robert W. Layman†

Lewis Research Center

SUMMARY

The HIP-1 hot ion plasma was a steady-state $\vec{E}\times\vec{B}$ discharge contained in a magnetic mirror geometry. The electrode geometry consisted of hollow cathodes placed on the magnetic axis and circular anodes concentric with the cathodes. The anodes and the cathode tips were located near the mirror throats. The discharge was operated with grounded anodes and with cathode voltages to -22 kilovolts. The HIP-1 plasma produced hydrogen ion temperatures up to 900 electron volts and with deuterium gas steady-state neutron activity of about 10^6 neutrons per second. Initial results are presented for two additional diagnostic procedures on HIP-1: (1) neutron diagnostics to determine where neutrons originated within the plasma discharge chamber and (2) electrode calorimetry to measure the steady-state power absorbed by the anodes and cathodes. Initial results are also reported for a hot-ion plasma formed with a continuous-cathode rod, one that spans the full length of the test section, in place of the two hollow cathodes.

The outboard neutron source strength increased relative to that at the midplane when (1) the cathode tips were moved farther outboard, (2) the anode diameters were increased, and (3) one of the anodes was removed. The distribution of neutron sources within the plasma discharge chamber was insensitive to the division of current between the two cathodes. For the continuous cathode, increasing the discharge current increased the midplane neutron source strength relative to the outboard source strength.

Each cathode absorbed from 12 to 15 percent of the input power regardless of the division of current between the two cathodes. The anodes absorbed from 20 to 40 percent of the input power. The division of power absorption between the two anodes varied with plasma operating conditions and electrode placement.

---

*Presented at American Physical Society meeting, San Francisco, California, November 15-19, 1976.

†Research Associate, Dartmouth College, Hanover, New Hampshire.

INTRODUCTION

HIP-1 is a steady-state, water-cooled magnetic mirror facility with a mirror ratio of 1.82 and a maximum magnetic field of 2.15 teslas at the mirrors (refs. 1 to 3). It was constructed at the NASA Lewis Research Center to develop a hot-ion plasma source for use in thermonuclear research. A steady-state plasma was formed by applying a radially inward dc electric field. The electrode geometry consisted of hollow cathodes placed on the magnetic axis and circular ring anodes concentric with the cathodes. Both the cathode tips and the anodes were located near the mirror throats. The cathodes and anodes were water-cooled. The perpendicular electric and magnetic fields caused the plasma to rotate ($\vec{E}\times\vec{B}$ drift) in the azimuthal direction (ref. 4). This azimuthal motion provided a kinetic energy input, predominantly to the ions. Randomization of this directed ion motion, that is, ion heating, may have been due primarily to oscillations (refs. 5 and 6). Hydrogen ion temperatures up to 900 electron volts have been measured in the HIP-1 plasma (ref. 7). In experiments conducted in the Superconducting Magnetic Mirror Apparatus (SUMMA) at Lewis (refs. 8 to 10), this same plasma heating process produced ion temperatures in the kilovolt range for hydrogen and helium plasmas.

HIP-1 plasma scaling relations were empirically obtained for the dependent variables, discharge current, ion temperature, electron temperature, and relative ion density, as a function of the independent variables, gas flow rate, magnetic field, and cathode voltage (ref. 3). Steady-state neutron yields from the HIP-1 deuterium plasma were estimated (by neutron counting techniques) at about 10^6 neutrons per second. It was not established whether the neutrons came from the plasma volume or from the surfaces of the electrodes and test section or from both.

The purpose of this report is to present the initial results from two additional diagnostic procedures on the HIP-1 system: (1) neutron monitoring experiments to determine the distribution of neutron sources within the plasma discharge chamber and (2) electrode calorimetry to measure the steady-state power absorbed by the cathodes and anodes.

The electrode geometry has been modified to achieve greater reliability and more efficient plasma production. The most notable modification was that the electrically floated shields (ref. 3) were changed from water-cooled metal plates to uncooled boron nitride disks. Finally, this report also presents the results of plasma operation with a continuous-cathode rod that spanned the length of the test section.

For all plasma results reported, deuterium gas was used, and the midplane magnetic field was 0.9 tesla.

EXPERIMENTAL APPARATUS AND PROCEDURE

A schematic view of the plasma test section and magnet configuration is shown in

figure 1. The test section was a water-cooled cylinder made of 304 stainless steel. It was 25 centimeters in diameter and 1.63 meters in length. Diffusion pumps at each end of the test section evacuated it to a base pressure of about 6.7×10^{-5} newton per square meter (5×10^{-7} torr). At each end port, a quartz window provided a good view of the plasma and electrodes. The midplane ports provided access for visual observation of the plasma and for diagnostic instrumentation such as an optical monochromator and a Langmuir probe system.

A schematic of the electrode circuit is given in figure 2. The high-voltage power supplies (rated at 10 kV, 10 A each) were connected in series and operated up to 23 kilovolts. An on-off high-voltage vacuum switch was operated remotely from the control room. The cathode currents were measured with electrically floated ammeters. The anodes were grounded through 1-ohm resistors. The anode current was proportional to the measured voltage drop across the grounding resistors.

Electrode Assembly

The locations of the anodes, cathodes, and boron nitride shields are shown in figure 1. The electrode assembly is shown in figure 3. This assembly differed in several ways from the water-cooled electrodes used previously in HIP-1 (ref. 3). The features of the new electrode assembly were (1) an uncooled boron nitride disk (15.2-cm diam and 1.27-cm thickness) replaced the metal, water-cooled, electrically floated shield; (2) the cathode outside diameter was 2.86 centimeters along its entire length; (3) the gas feed hole in the cathode was a constant-diameter (1.27-cm) tube that extended the full length of the cathode; (4) the high-voltage insulator was inverted so that the metal-to-ceramic joint was on the outside rather than on the inside of the test section; and (5) a metal bell-shaped housing was placed around the outside of the high-voltage insulator to reduce corona discharge.

A metal, electrically floated shield had been used in all previous plasma heating experiments in both HIP-1 (refs. 1 to 3) and SUMMA (refs. 8 to 10). The shield served two main purposes: (1) it protected the high-voltage, ceramic, cathode-feedthrough insulator from plasma bombardment, and (2) it prevented direct arcing along magnetic field lines from the cathode to the grounded back flange. There was, however, a discharge in the annular gap between the cathode and the floated shield because the shield was at a higher potential than the cathode. This discharge was a leakage path from the cathode to the shield and then to either the grounded back flange or the anode or to both. The floated, metal shield also formed its own reflex discharge. The boron nitride disk was substituted for the metal shield to eliminate these leakage currents to ground.

Exceptionally stable plasma operation was achieved for voltages and currents to -23 kilovolts and 1 ampere, respectively. Anode and cathode currents were equal,

which meant there was no leakage current to ground. At the higher voltages and at discharge currents above about 1 ampere, the uncooled, boron nitride disks were heated to about 800° C.

The water-cooled anodes were helixes wound with two loops of copper tubing. They were not coated with tungsten as were previous anodes (ref. 3) because they did not sputter excessively for the range of discharge parameters covered in this work. Except for one run with the continuous cathode, the anode inside diameter was 5 centimeters. The copper cathodes were flame sprayed with a tungsten coating because they sputtered appreciably.

Neutron Monitoring System and Calibration Procedure

The boron fluoride (BF_3) neutron counter described in reference 3 was used in these experiments. While good for measuring the integrated neutron output, BF_3 counters are not easily applied to the measurement of local neutron production. However, by the method described in this section the BF_3 counters were made useful for studying the axial distribution of neutron sources in the machine.

Five Geiger tubes were wired in parallel and embedded in a block of paraffin 20 by 20 by 30 centimeters (fig. 4). The paraffin block was covered with cadmium foil to reduce the probability of counting scattered neutrons. The output of the Geiger tubes went to a preamplifier and then to a scaler. A timer gated the scaler on for a preset timing interval, which was usually 100 seconds. The neutron counts ranged from 300 to over 10 000 for this timing interval, depending on the plasma operation conditions.

The neutron monitoring setup is shown in figure 5. The Geiger counter assembly was placed on a bench that was located directly beneath and alined parallel to the test section axis. The counter could be slid along the bench to count neutrons at various axial positions. Neutrons were counted at 11 standard counter positions along the bench: 0, ±12.7, ±25.4, ±38.1, ±50.8, and ±57.2 centimeters.

A californium 252 neutron source of known activity was used to obtain the neutron-scattering characteristics of the HIP-1 facility. With this neutron source located at a given position on the test-section axis, neutrons were counted at the 11 standard bench positions. Eleven plots of the neutron count rate as a function of axial position along the bench, or the axial distribution of neutron counts, were obtained, one for each of 11 neutron source positions equally spaced along the test-section axis. These source positions were at 0, ±12.7, ±25.4, ±38.1, ±50.8, and ±63.5 centimeters along the test-section axis.

When the principle of linear superposition is applied to these 11 neutron-scattering calibration curves, a composite axial distribution of neutron counts can be obtained for any arbitrary combination of the 11 sources. The composite count at a given counter

position is the sum of the counts produced by each source, taken one at a time. The HIP-1 calibration curves of figure 6 were obtained by linear superposition of the neutron counts produced by each of the neutron sources whose axial locations are given for the curves. The sources were of equal activity, and the neutron count rate was normalized to 1000 at the midplane.

Electrode Calorimetry

Electrode calorimetry consisted of measuring water-flow rates to the electrodes and using differential thermocouples to measure the temperature rise of the water. A schematic of the calorimetry setup is shown in figure 7. The cathode water-coolant lines had an equivalent resistance of approximately 1 megohm to ground. The ohmic heating of the cooling water was experimentally measured and subtracted from the cathode calorimetry results. The leakage current through the cathode water lines was subtracted from the measured cathode current.

Figure 8 includes a sketch of the general anode-cathode arrangement used for this report and a listing of the electrode configurations tested and the measurements made for each test series.

DISCUSSION OF RESULTS

In reference 3, two modes of operation were identified from the current-voltage (I-V) discharge characteristics. In the low-voltage region (typically <10 kV) the plasma currents were high and increased rapidly with cathode voltage, and the discharge was unstable. This mode was termed the low-resistance operating mode. At higher voltages (>10 kV) the currents were lower and almost independent of cathode voltage, and the discharge was stable. This mode was termed the high-resistance operating mode. Hydrogen ion temperatures as high as 900 electron volts were generated in HIP-1 during operation in the high-resistance mode (ref. 7). Operation in the high-resistance mode was characterized by a visible halo that surrounded the plasma at the midplane. All experimental data presented in this report were obtained for the high-resistance operating mode.

Current-Voltage Characteristics

When the neutron monitoring results and the electrode calorimetry results are discussed, the I-V characteristics of the discharge are needed. Therefore, the I-V

characteristics are discussed first. For fixed cathode voltage, the current drawn by a hollow cathode was controlled by the amount of gas that flowed through it. However, the current drawn by each individual anode was not directly controllable. Repositioning of the cathodes had some effect on the anode current distribution. There was, however, no way to realine anodes and cathodes with the system under vacuum. Anode alinement with respect to the magnetic field lines may have a strong effect on the formation of anode sheaths and in turn affect the distribution of anode currents.

Figure 9 presents the I-V characteristics for three different anode-cathode configurations. For the results of figure 9(a), the tips of the cathodes were 5 centimeters outboard with respect to the inboard face of the anodes. The west cathode, which had the higher gas flow, drew more current than did the east cathode. The anode currents were very well balanced for this case. The currents increased slightly with increasing cathode voltage. The sum of the cathode currents was approximately equal to the sum of the anode currents, which indicates that leakage currents to ground were eliminated with the new electrode design.

Figure 9(b) shows the results for the configuration with the cathode tips placed flush with the inboard face of the anodes. The cathode gas flows were adjusted to give approximately equal cathode currents. The east anode current was about twice the west anode current. The anodes were in exactly the same position for both figures 9(a) and (b).

Figure 9(c) shows the results for single-anode operation. The curves on the left are for gas feed to the west cathode only, and those on the right are for gas feed to the east cathode only. The cathode that had no gas flow drew very little current (~0.04 A), and this current did not vary with the cathode voltage. As shown in figure 9(c), the anode current was independent of whether gas flowed into the east or the west cathode.

Neutron Monitoring

The purpose of these neutron monitoring experiments was to obtain knowledge of the distribution of neutron sources within the plasma discharge chamber. Ideally, the neutron calibration curves (fig. 6) could be weighted and combined by the principle of superposition to give a best fit to the measured axial distribution of neutron counts. To apply superposition, it would be necessary to assume that the neutrons originated on the axis of the system and that the plasma parameters stayed constant over the several hours of continuous operation needed to obtain good statistics. Since these assumptions were questionable, the superposition technique was not attempted. Instead trends that emerged in the measured axial distribution of neutron counts as certain electrode parameters were systematically varied were compared with the trends expressed in the family of neutron calibration curves of figure 6.

Hollow cathode. - Figure 10 illustrates the effect of varying the axial position of the cathode tips. A comparison of figure 10 with figure 6 suggests that, as the cathode tips were moved outboard from ±31 to ±54 centimeters, the main source of neutrons moved outboard. For the case where the cathodes were positioned nearer the midplane (i. e., the ±24- and the ±31-cm curves) it might be argued that there were two main sources of neutrons, one near the midplane (indicated by the bump in the middle) and another farther outboard (giving rise to the wings).

Figure 11 shows the axial distribution of counts for three different anode positions and a fixed cathode position. These curves do not suggest a strong effect of anode position on the distribution of neutron sources.

Figure 12 shows the axial distribution of neutron counts for single- and double-anode operation. For single-anode operation, the anode on the east side was removed. On the west side of the midplane, the axial distribution was nearly the same for both single- and double-anode operation. On the east side of the midplane, the normalized neutron count rate was higher for single-anode operation than for double-anode operation.

For single-anode operation, figure 12 also compares results for gas feed into the west cathode only with results for gas feed into the east cathode only. On the east side of the midplane, the neutron production was only slightly higher when gas was fed exclusively into the east cathode than when gas was fed exclusively into the west cathode. Thus, the axial distribution of neutron sources did not depend on the relative amounts of gas that flowed through each cathode. These results suggest that the dominant neutron production near the ends was not due to fusion collisions of fast ions with neutrals that emerged from the cathode tips. Further, these results suggest that neutron production should not be attributed to the additional cathode current that accompanies the introduction of gas through the hollow cathodes.

Figure 13 is another plot that shows how the axial distribution of neutron counts was affected when the cathode tip position was changed relative to a fixed anode. These results are included for completeness because they were obtained from the same electrode configurations that were used for several other studies whose results are described in this report. These include (1) the I-V results of figures 9(a) and (b), (2) the electrode calorimetry results presented in figures 17 and 18, and (3) some of the results discussed in the section Qualitative Observations of HIP-1 Plasma.

Figure 13 reveals that when the cathode tips were moved from ±31 to ±38 centimeters the following occurred: (1) the outboard neutron count rate increased relative to the midplane count rate (which is the same trend shown in fig. 10), (2) the total gas flow rate was increased from 0. 25 to 0. 40 cubic centimeter per second (at standard temperature and pressure (STP)) in order to maintain the same total current, (3) the midplane neutron count rate more than doubled. This last result indicates that the neutron count rate depends on gas flow rate (or test-section pressure) rather than on discharge current.

Continuous-cathode rod. - In an attempt to clarify the effects of the hollow-cathode

gas feed on the operation of the plasma discharge, the two hollow cathodes were replaced by one cathode rod that spanned the test-section length. This continuous-cathode rod was located on the test-section axis. The anodes were located at ±16 centimeters on this particular occasion. The gas was fed in at the top of the test section at the midplane.

Compared with the hollow-cathode discharge, the continuous-cathode discharge required higher gas flow rates for the same current and had a steeper slope for its current-voltage curve.

The continuous-cathode plasma discharge is shown in figure 14. At the midplane can be seen the vertical stripe, termed a halo, that characterized the high-resistance mode of the hollow-cathode discharge (ref. 3). On the one occasion when the continuous-cathode rod was inadequately cooled, it overheated and structurally failed at the midplane. The burst copper cathode tube is shown in figure 15. The surface of the continuous-cathode tube was sputtered directly underneath each anode and also over a 15-centimeter length about the midplane. The sputtering and overheating at the midplane and the neutron data discussed in the next paragraph all offer consistent evidence that the continuous-cathode plasma was very energetic at the midplane.

Figure 16 shows the axial distribution of neutron counts for the continuous-cathode plasma. At the lower currents (~0.2 A), there were neutron sources both near the midplane and farther outboard. The figure suggests a stronger outboard source of neutrons (relative to the midplane source) for the 7.6-centimeter-diameter anode than for the 5.1-centimeter-diameter anode. Figure 16 also suggests that, as the current increased (for the 5.1-cm-diam anode), the neutron activity became strongest near the midplane. This effect of current on neutron source distribution should also be examined for the hollow-cathode operation.

The results from the hollow-cathode and the continuous-cathode tests indicate that the outboard source of neutrons increased relative to the midplane source when (1) the anode diameter was increased, (2) an anode was removed, and (3) cathodes were moved farther outboard.

Electrode Calorimetry

Calorimetry is essential for plasma power balances, and it should also be helpful for electrode-sheath studies. At present, the calorimetry on HIP-1 is limited to the measurement of steady-state power absorbed by the cathodes and anodes. The initial results of these electrode power absorption measurements are reported in this section.

Figure 17 shows the fraction of input power absorbed by the electrodes as a function of cathode voltage for the cathode tips placed outboard of the anodes. Figure 9(a) gives the I-V characteristics that correspond to the calorimetry data of figure 17. Each cath-

ode absorbed equal power despite the fact that the west cathode carried twice the current of the east cathode. The west anode absorbed a constant fraction of input power at all cathode voltages. The fraction of input power absorbed by the east anode varied from twice that of the west anode at high voltage to approximately the same value at low voltages. The trends of anode current as a function of voltage (fig. 9(a)) are similar to the anode power absorption trends. The individual anode currents, however, are closer in magnitude over the entire voltage range than are the individual anode power fractions.

Figure 18 shows the fractional power absorbed as a function of cathode voltage for the configuration with the cathode tips flush with the inboard face of the anodes. Figure 9(b) gives the I-V characteristics that correspond to the calorimetry data of figure 18. Again, as in figure 17, the east and west cathodes each absorbed approximately equal power, but in this case both cathode currents were equal. The fraction of input power absorbed by the west anode was again constant, but its value was only 0.045. Although the east anode absorbed less than 20 percent of the total anode power, it carried about 35 percent of the total anode current.

Figure 19 gives the power absorption results for one-anode operation with gas feed either into the west cathode only or into the east cathode only. Figure 9(c) gives the I-V characteristics corresponding to the data of figure 19. Again, as in figures 17 and 18, both the east and west cathodes each absorbed equal power. Furthermore, the cathodes each absorbed equal power regardless of which cathode the gas flowed through. And since the cathode current is related to the gas flow, each cathode absorbed equal power regardless of whether 85 percent of the cathode current flowed in the west or in the east cathode. It is also interesting to recall from figure 12 that for this electrode configuration the distribution of neutron sources was essentially the same regardless of which cathode the gas flowed through.

The cathode power results in figures 17 to 19 suggest that most of the power absorbed by the cathode did not come from the additional cathode current that accompanies the introduction of gas through the hollow cathode.

Figure 20 shows the effect of discharge current on electrode power absorption for one-anode operation. Both cathodes again absorbed equal power for all currents, and the anode absorbed about 40 percent of the input power.

Qualitative Observations of HIP-1 Plasma

When HIP-1 was operated with cathode voltages above 18 kilovolts and discharge currents above 0.5 ampere, parts of the electrode system and the test section were heated sufficiently to be hot to the touch or to glow red-hot. These observations of heating and their possible significance are summarized in this section.

For double-anode operation, (1) with the cathode tips placed 5 centimeters outboard

from the anode, both boron nitride disks were equally heated to a red-hot condition, and the midplane viewing-port windows were at room temperature; (2) with the cathode tips flush with the inboard anode faces, both boron nitride disks were dark, but the midplane viewing ports and their windows were very hot to the touch. For single-anode operation, the boron nitride disk at the end where the anode was removed glowed red-hot, while the opposite boron nitride disk was dark.

These results indicate that, where an anode was removed or where the space between the anode and the cathode tip was increased, more plasma flowed toward that end of the machine. One possible explanation is simply that these procedures reduced the physical blockage by the anodes. On the other hand, both of these procedures might have weakened the radial electric fields in the magnetic mirror regions. This might constitute evidence that strong radial electric fields near the mirror throats enhanced plasma containment.

CONCLUDING REMARKS

Initial results were reported for two additional diagnostic procedures on HIP-1, namely, neutron monitoring and electrode calorimetry. These were used to study the plasma under a variety of operating conditions and anode-cathode geometries; they proved to be useful techniques.

An axial distribution of the neutron count rate was obtained for each of 11 neutron source positions along the test section axis. These results were combined by superposition to yield a family of calibration curves for the neutron scattering characteristics of the HIP-1 facility. The measured axial distribution of the neutrons for the HIP-1 plasma was compared with the calibration curves. This procedure provided insights into the distribution of neutron sources within the plasma discharge chamber.

The steady-state power absorbed by the anodes and cathodes was obtained by measuring the flow rate and temperature rise of the water coolant.

This report also presented the results of plasma operation with a continuous cathode, a single cathode rod that spanned the length of the test section. Very strong heating and sputtering of the cathode rod at the midplane gave good evidence that energetic ions were present at the midplane.

SUMMARY OF RESULTS

The following results were obtained in neutron monitoring and electrode calorimetry experiments in the HIP-1 hot ion plasma:

1. The cathodes experienced strong sputtering, while the anodes did not.

2. The gas flow through a hollow cathode controlled the current drawn by that cathode. With gas feed into one cathode only, that cathode carried 85 percent of the total cathode current.

3. Each cathode absorbed about 0. 12 to 0. 15 of the input power. This fraction was independent of the current drawn by the cathode.

4. The ratio of power absorbed by one anode to that absorbed by the other anode varied from 0. 17 to 0. 5. However, the fraction of the total anode power absorbed by a given anode was not equal to the fraction of total current drawn by that anode.

5. The division of current between the two cathodes did not strongly influence the axial distribution of neutron sources within the discharge chamber.

6. The outboard source of neutrons increased relative to the midplane source when (1) the anode diameter was increased, (2) an anode was removed, and (3) the cathodes were moved farther outboard.

7. Some of the results lead to the following speculation about the HIP-1 plasma: Hot ions from the main body of plasma escaped out the ends and struck the cathode tips. As these ions moved axially outward through a region of decreasing potential, they acquired additional axial energy. These energetic ions accounted for the cathode heating and sputtering and possibly the outboard source of neutrons. These ions also accounted for the minimum current drawn by the hollow cathode when its gas flow was shut off. When gas flowed through the cathode, an ionized gas region was formed near the cathode tip which provided for increased electron emission into the plasma and increased ion flow to the cathode.

Lewis Research Center,
National Aeronautics and Space Administration,
Cleveland, Ohio, February 9, 1977,
506-25.

REFERENCES

1. Sigman, Donald R.; and Reinmann, John J.: Steady-State Hot-Ion Plasma Produced by Crossed Electric and Magnetic Fields. NASA TM X-2783, 1973.

2. Sigman, Donald R.; Reinmann, John J.; and Lauver, Milton R.: Parametric Study of Ion Heating in a Burnout-Type Device (HIP-1). NASA TM X-3033, 1974.

3. Reinmann, J. J.; et al.: Hot Ion Plasma Production in HIP-1 Using Water-Cooled Hollow Cathodes. NASA TM X-71852, 1975.

4. Englert, G. W.; Reinmann, J. J.; and Lauver, M. R.: Interpretation of Neutral Particle Analyzer Measurements on Plasmas Having Azimuthal Drift. Plasma Phys., vol. 17, no. 7/8, July/Aug. 1974, pp. 609-621.

5. Thermonuclear Division Annual Progress Report for Period Ending December 31, 1971. ORNL 4793, Oak Ridge Nat. Lab., 1972, p. 33.

6. Hirose, A.; and Alexeff, I.: Electrostatic Instabilities Driven by Currents Perpendicular to an External Magnetic Field. Nucl. Fusion, vol. 12, no. 3, May 1972, pp. 315-323.

7. Lauver, M. R.: Effect of Anode-Cathode Geometry of Performance Characteristics of the HIP-1 Hot Ion Plasma. IEEE Int. Conf. on Plasma Science, 1976, p. 158.

8. Reinmann, J. J.; et al.: Hot Ion Plasma Heating Experiments in SUMMA. IEEE Trans. Plasma Sci., vol. PS-3, no. 1, Mar. 1975, pp. 6-14.

9. Reinmann, J. J.; et al.: NASA Superconducting Magnetic Mirror Facility. Fifth Symposium on Engineering Problems of Fusion Research. IEEE Nucl. Plasma Sci. Soc., 1973, pp. 587-591.

10. Reinmann, J. J.; et al.: SUMMA Hot Ion Plasma Heating Research at NASA Lewis Research Center. Sixth Symposium on Engineering Problems of Fusion Research. IEEE Nucl. Plasma Sci. Soc., 1975, pp. 423-429.

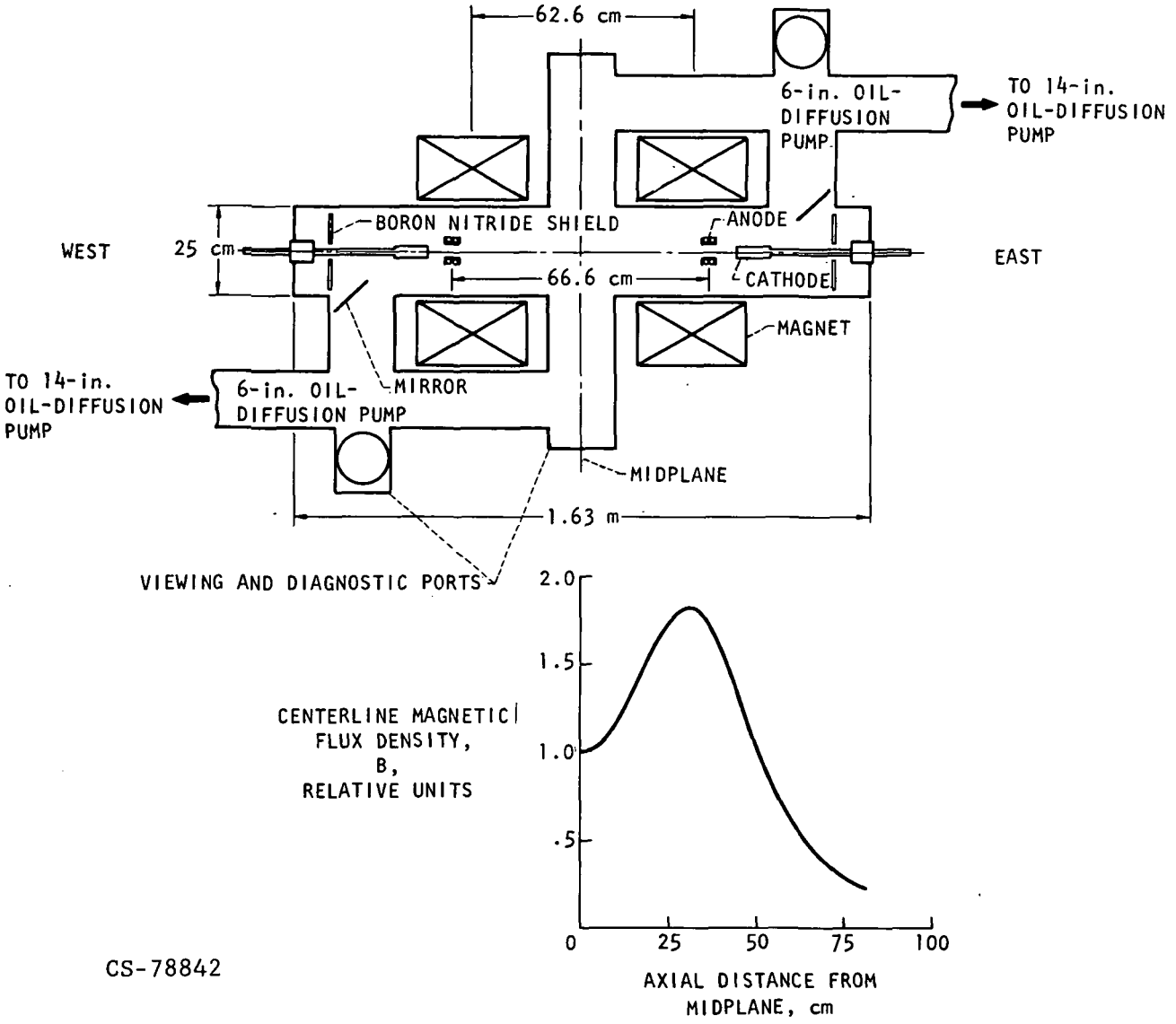

Figure 1. - Schematic view of HIP-1 test section and magnetic field configuration.

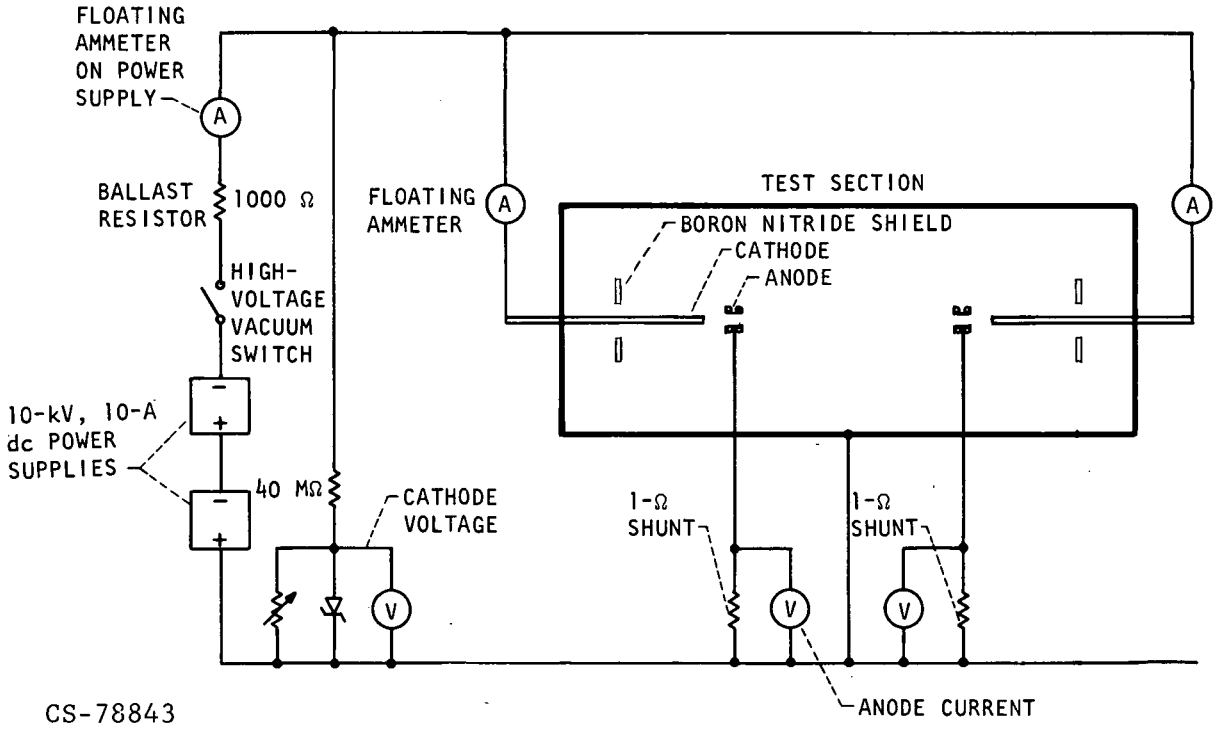

Figure 2. - Schematic of HIP-1 electrode circuit.

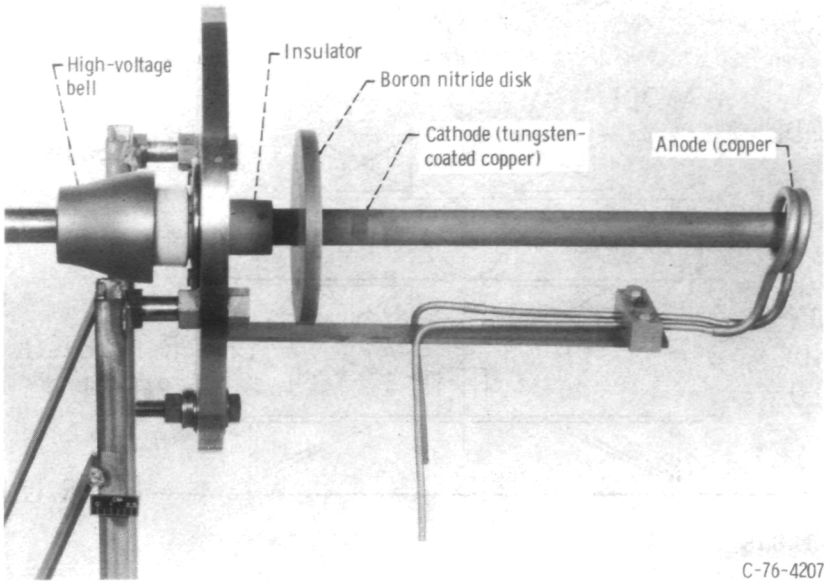

Figure 3. - HIP-1 electrode assembly.

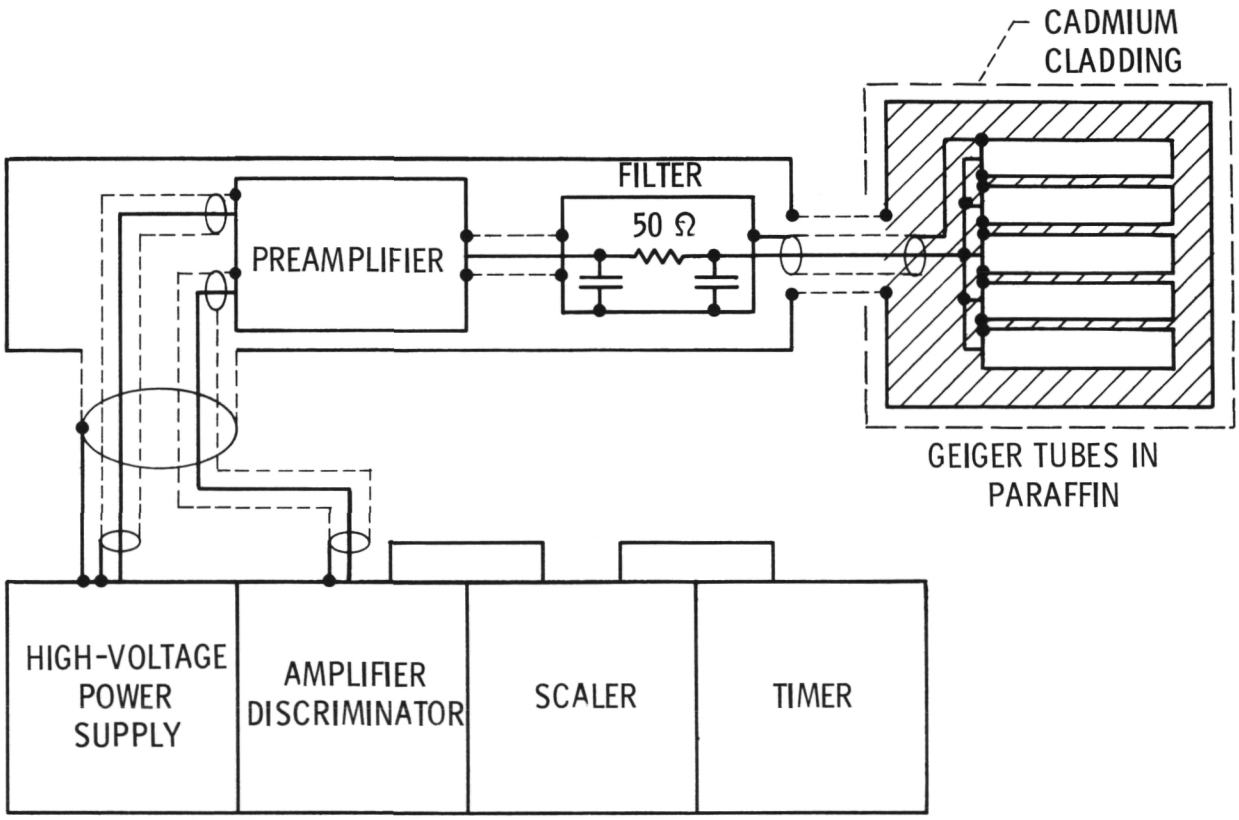

Figure 4. - Schematic of HIP-1 neutron instrumentation.

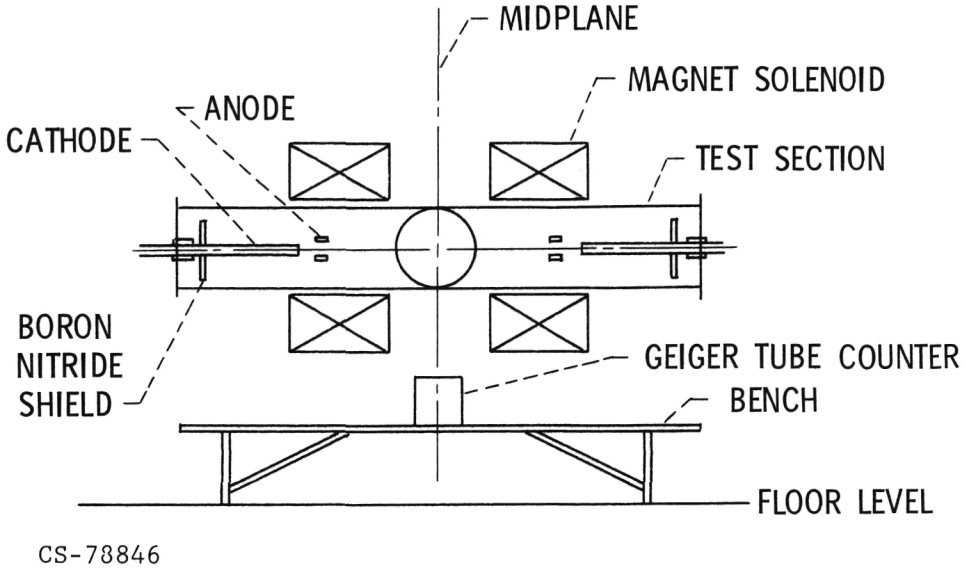

Figure 5. - HIP-1 neutron monitoring setup.

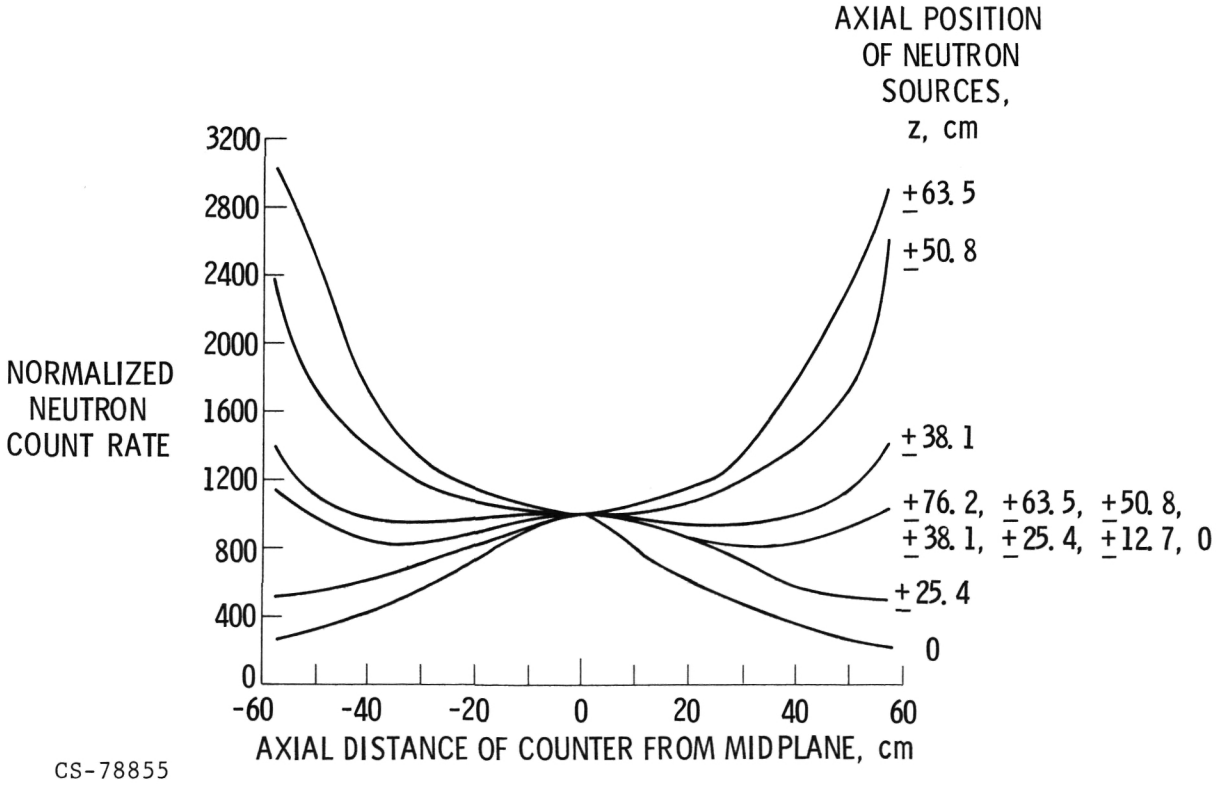

Figure 6. - Neutron scattering calibration curves for HIP-1.

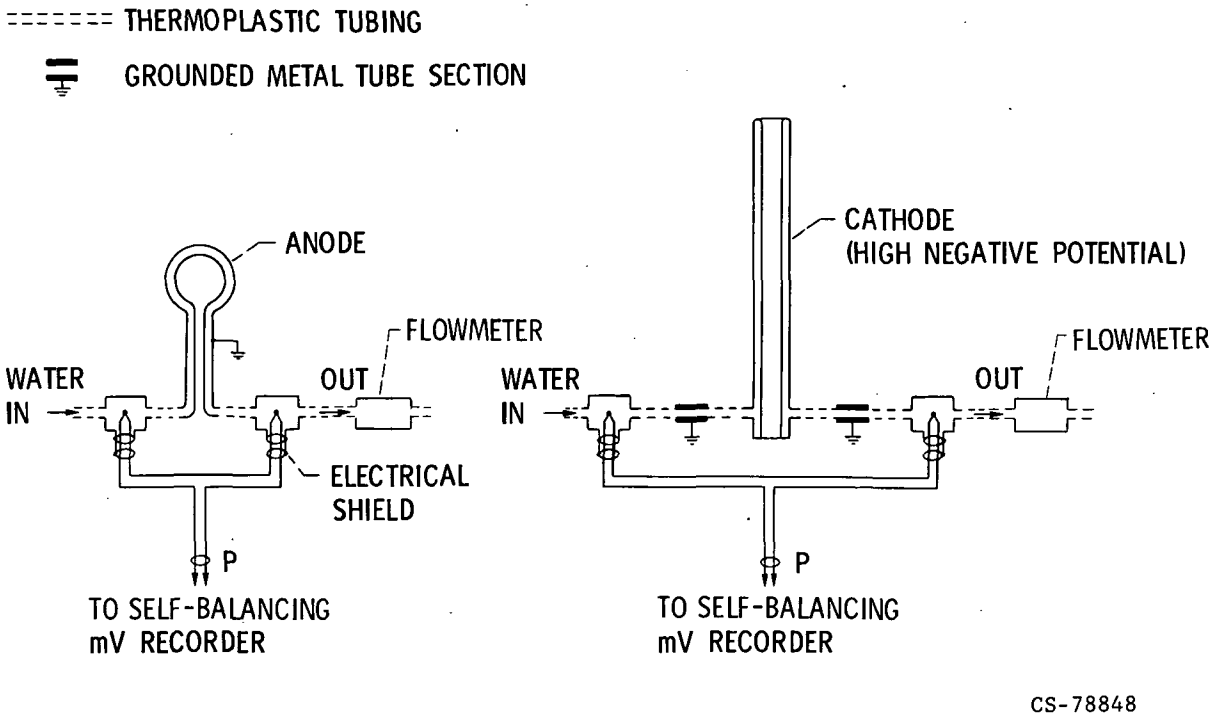

Figure 7. - Typical calorimetry setup for HIP-1 anodes and cathodes. Thermocouples electrically insulated from water.

DIMENSION, cm			CALORIMETRY	COMMENTS
w	x	y		
5	16	24	NO	----------
5	16	31		----------
5	16	41		----------
5	16	54		----------
5	31	31	YES	----------
5	31	38		----------
5	22	31		----------
5	31	31		EAST ANODE REMOVED
5	16	0		CONTINUOUS CATHODE
8	16	0		CONTINUOUS CATHODE

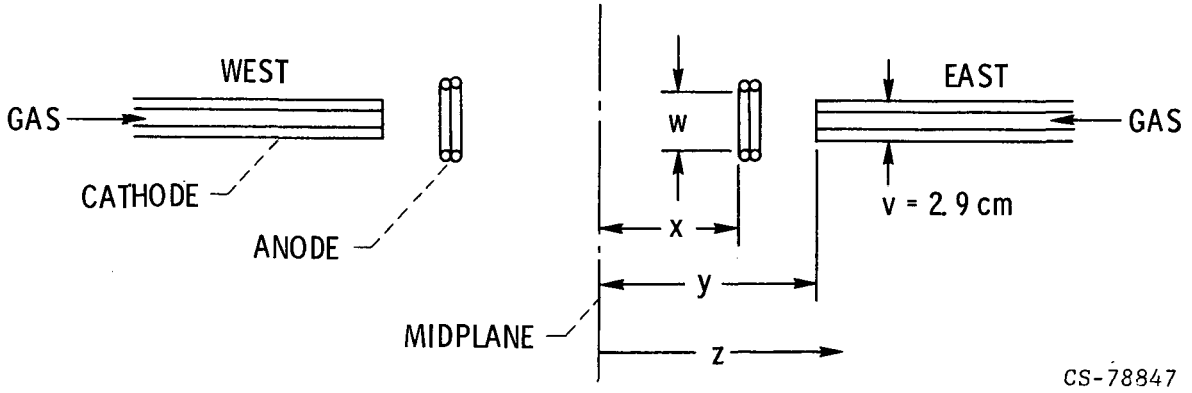

Figure 8. - Summary of HIP-1 electrode configurations studied. Counts as function of z were recorded for all configurations.

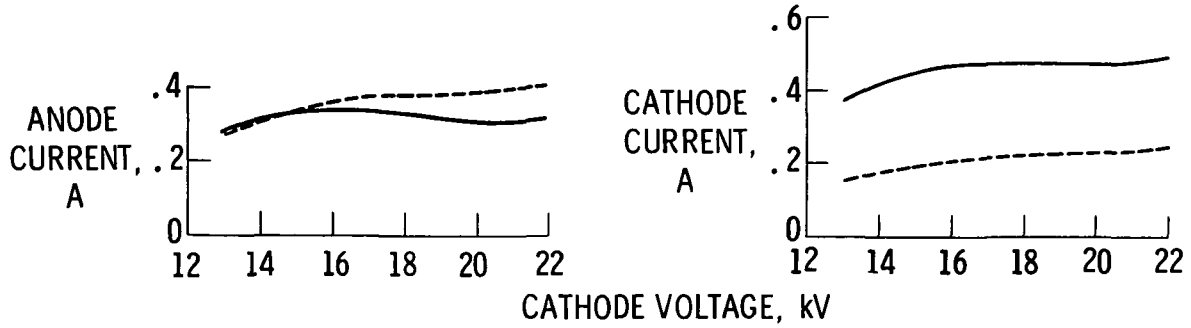

(a) Cathode tips placed outboard from anodes; cathode tips located at y = ±38 centimeters; anodes located at x = ±31 centimeters; west gas flow, 0.38 cubic centimeter per second (STP); east gas flow, 0.06 cubic centimeter per second (STP); midplane pressure, 1.7×10^{-2} newton per square meter (1.3×10^{-4} torr).

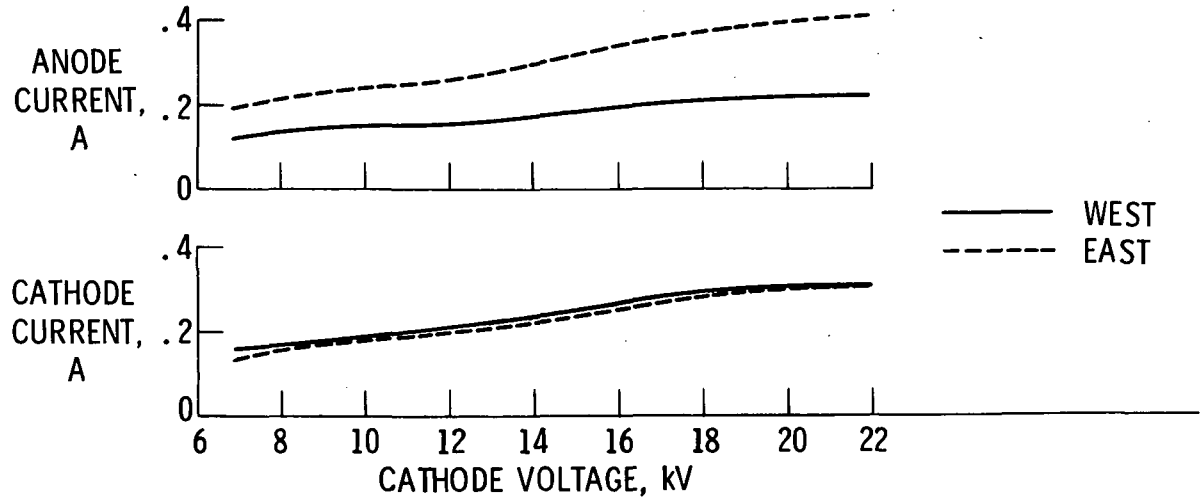

CS-78849

(b) Cathode tips flush with inboard face of anodes; cathode tips located at y = ±31 centimeters; anodes located at x = ±31 centimeters; west gas flow, 0.17 cubic centimeter per second (STP); east gas flow, 0.15 cubic centimeter per second (STP); midplane pressure, 1.2×10^{-2} newton per square meter (9×10^{-5} torr).

Figure 9. - Electrode current as function of cathode voltage. Anode diameter, 5 centimeters.

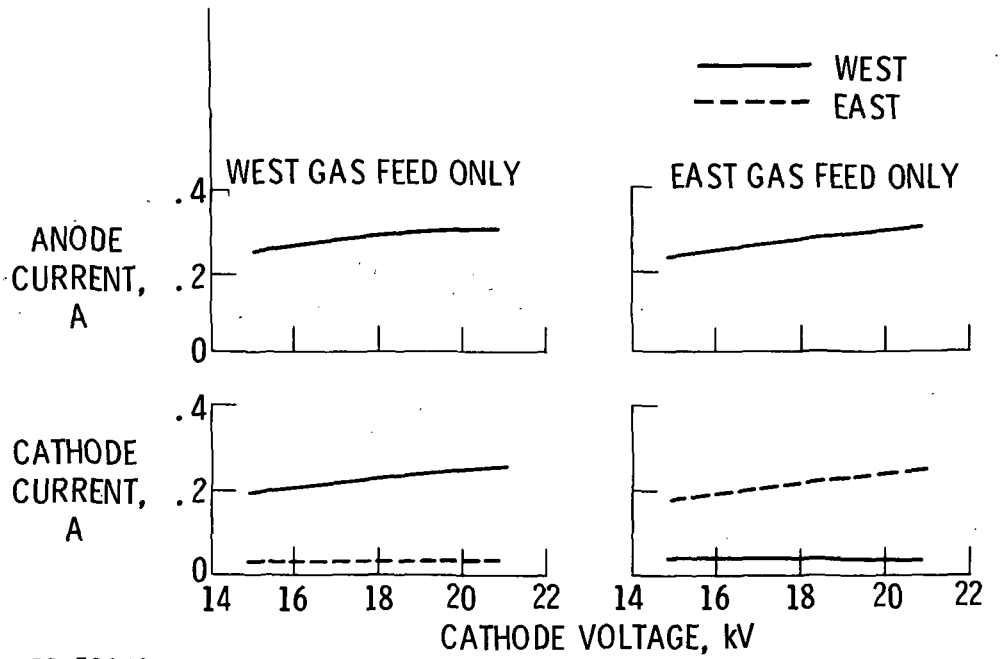

(c) Single-anode operation; cathode tips located at $y = \pm 31$ centimeters; anode located at $x = -31$ centimeters; midplane pressure, 1.1×10^{-2} newton per square meter (8.5×10^{-5} torr); gas flow for west gas feed only, 0.31 cubic centimeter per second (STP); gas flow for east gas feed only, 0.31 cubic centimeter per second (STP).

Figure 9. - Concluded.

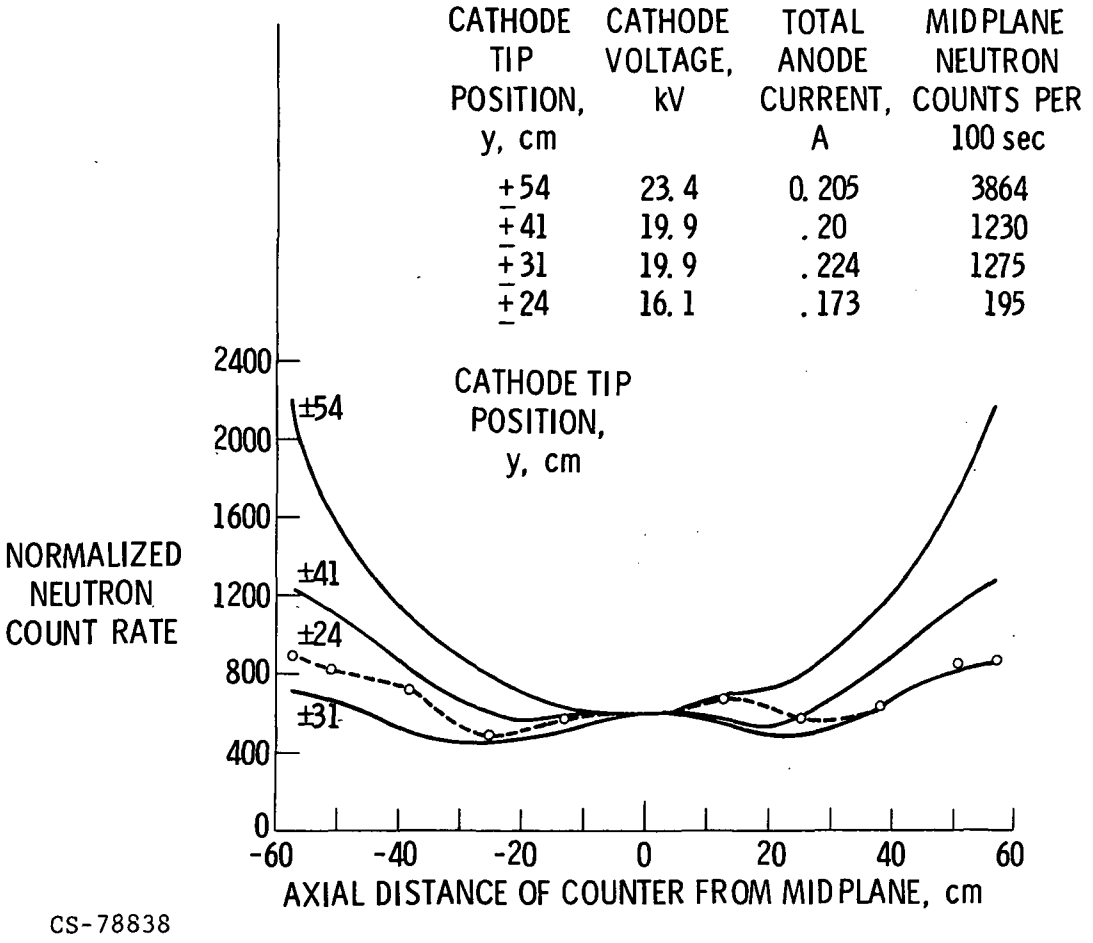

Figure 10. - Axial distribution of neutron counts for four cathode tip positions and one fixed anode position. Anodes located at $x = \pm 16$ centimeters; anode diameter, 5 centimeters.

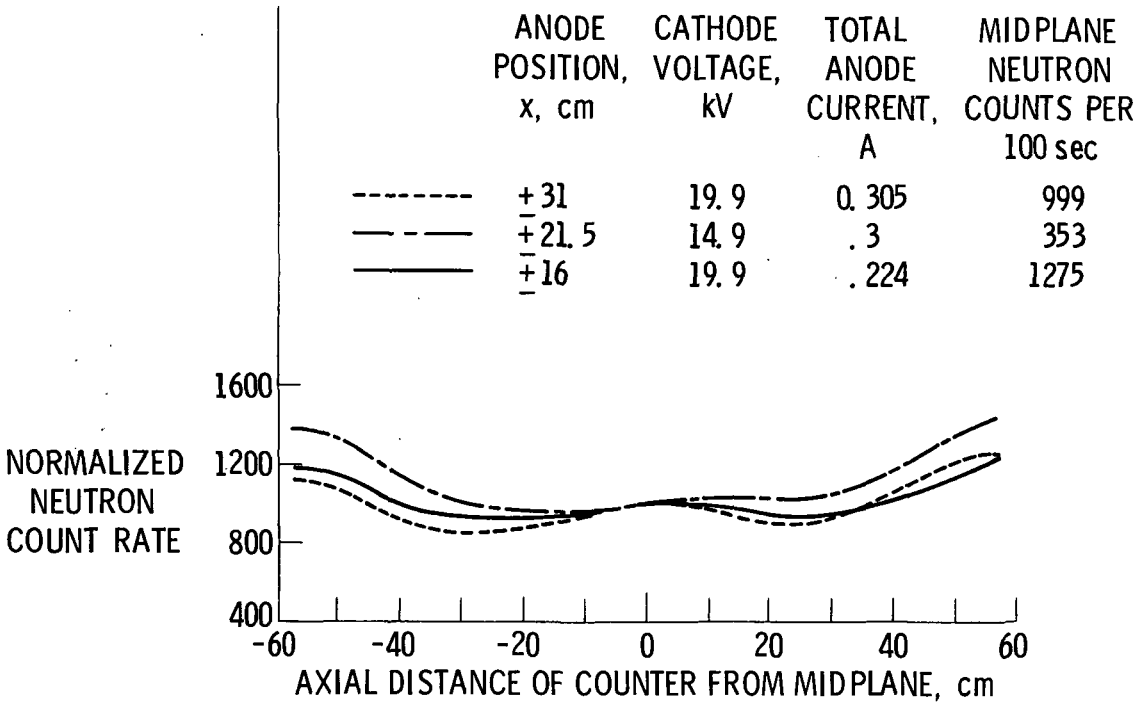

CS-78840

Figure 11. - Axial distribution of neutron counts for three anode positions and one fixed cathode tip position. Cathodes located at y = ±31 centimeters; anode diameter, 5 centimeters.

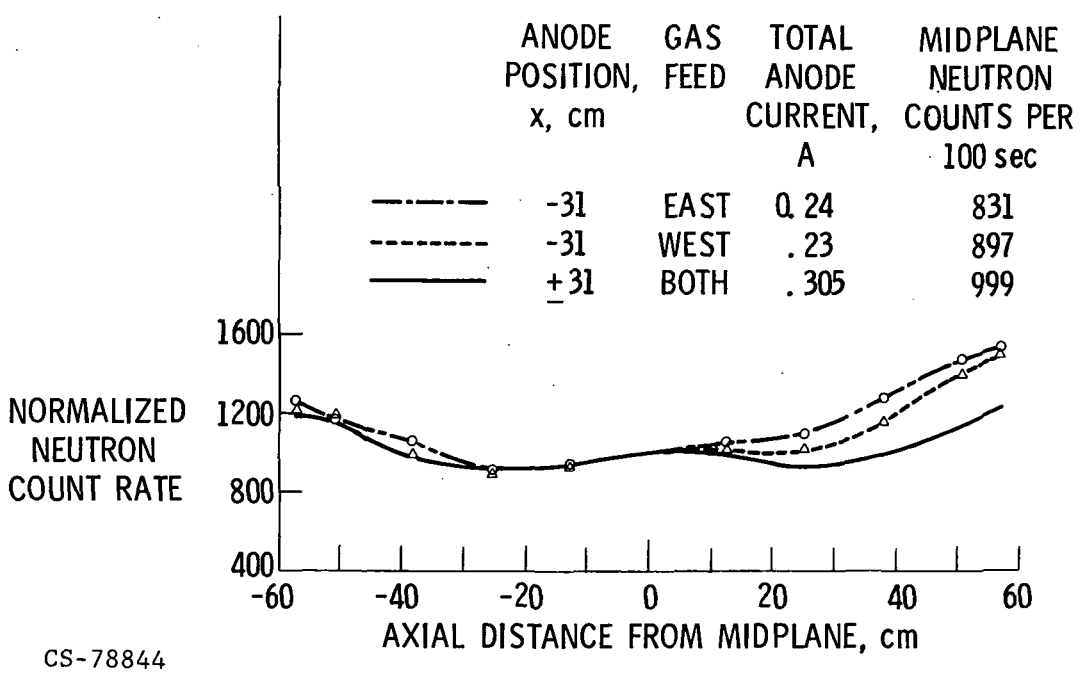

CS-78844

Figure 12. - Comparison of axial distribution of neutron counts for single- and double-anode operation. Cathode tips located at y = ±31 centimeters; anode diameter, 5 centimeters; cathode voltage, 19.9 kilovolts.

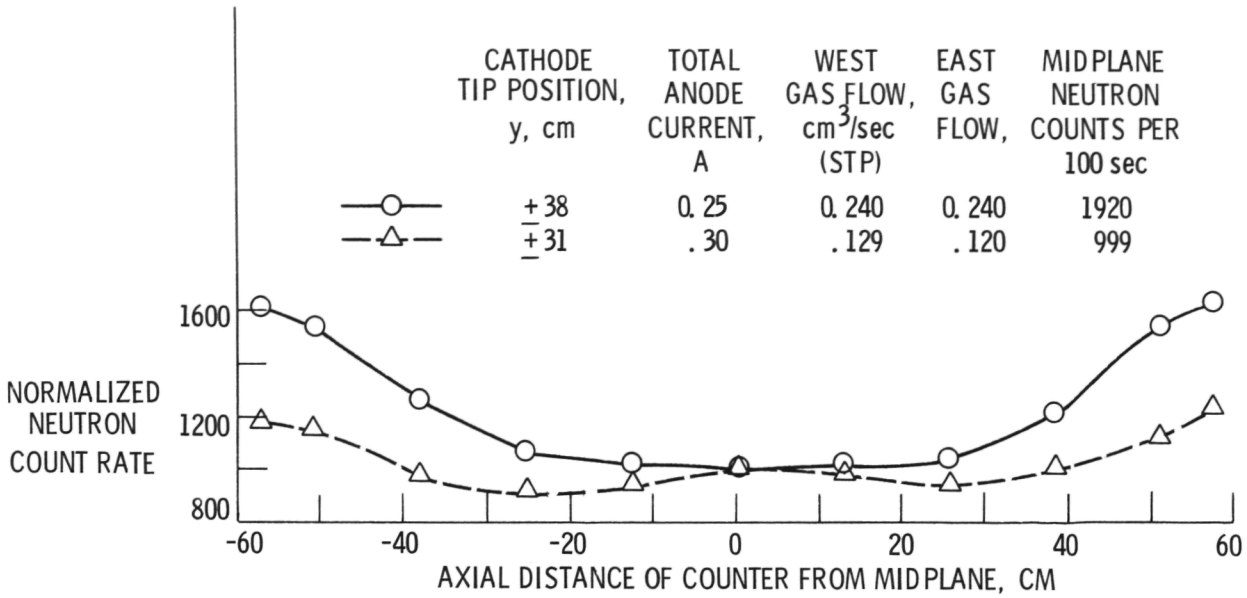

Figure 13. - Axial distribution of neutron counts for two cathode tip positions and one fixed anode position. Anodes located at x = ±31 centimeters; cathode voltage, 19.9 kilovolts.

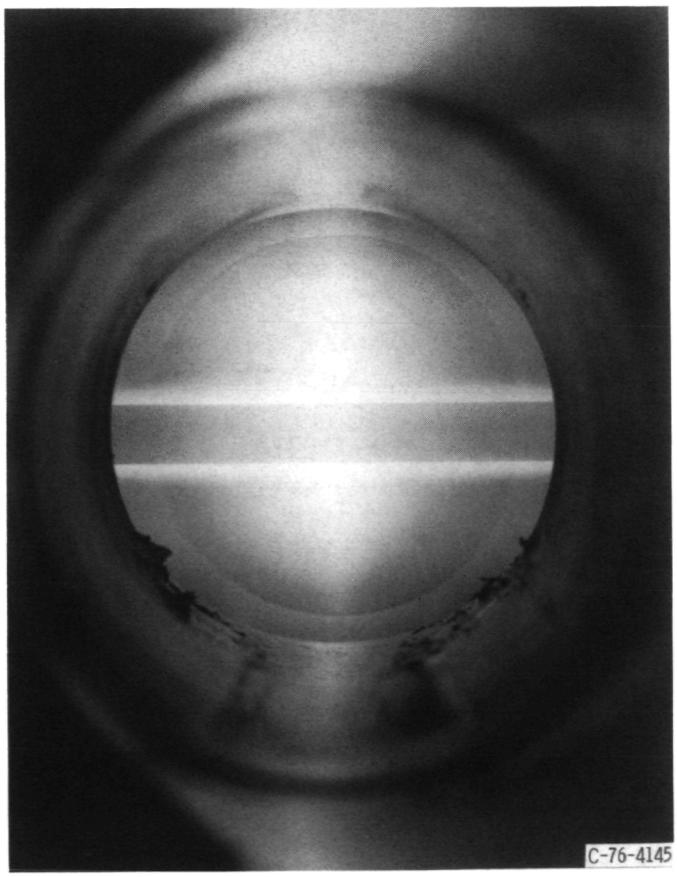

Figure 14. - Plasma formed with continuous cathode.

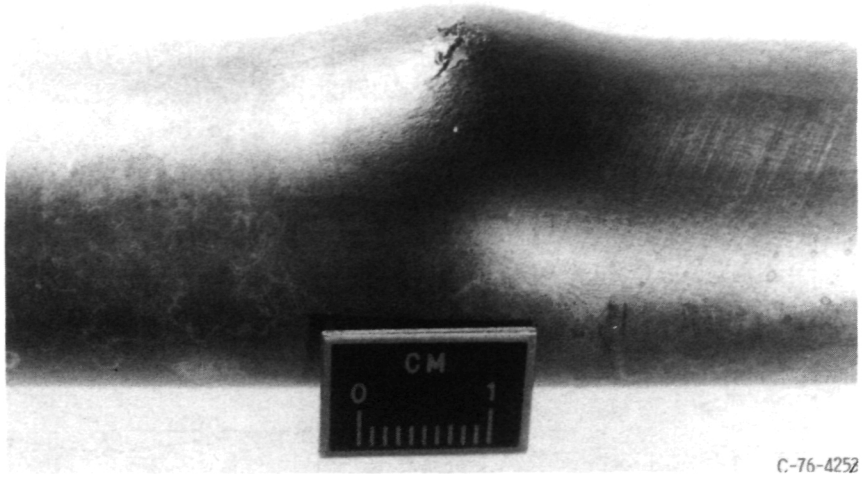

Figure 15. - Damage at midplane of continuous cathode.

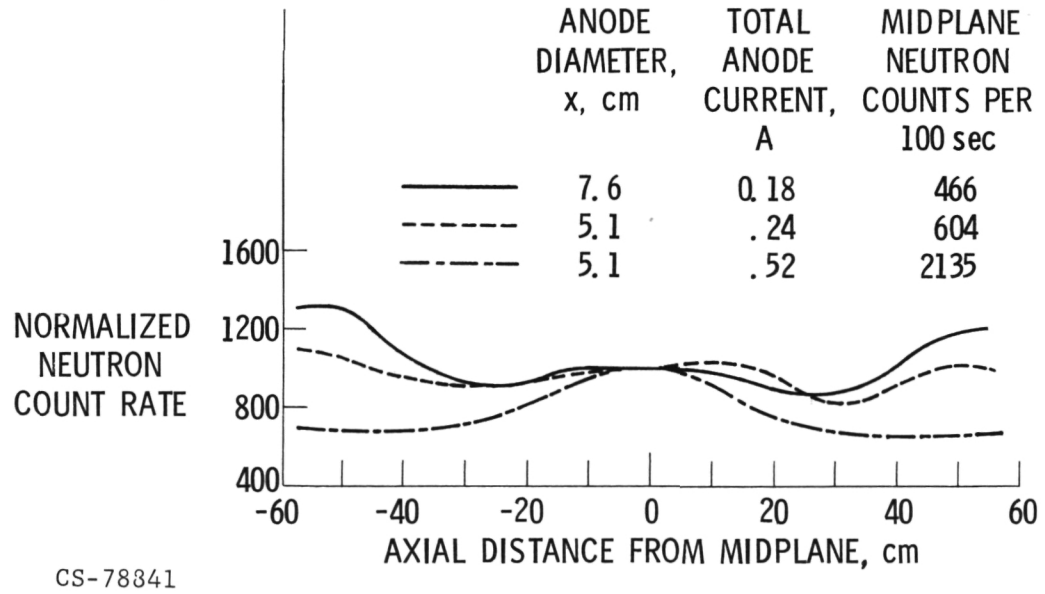

Figure 16. - Axial distribution of neutron counts for operation with continuous cathode. Anodes located at $x = \pm 16$ centimeters; cathode voltage, 19.9 kilovolts.

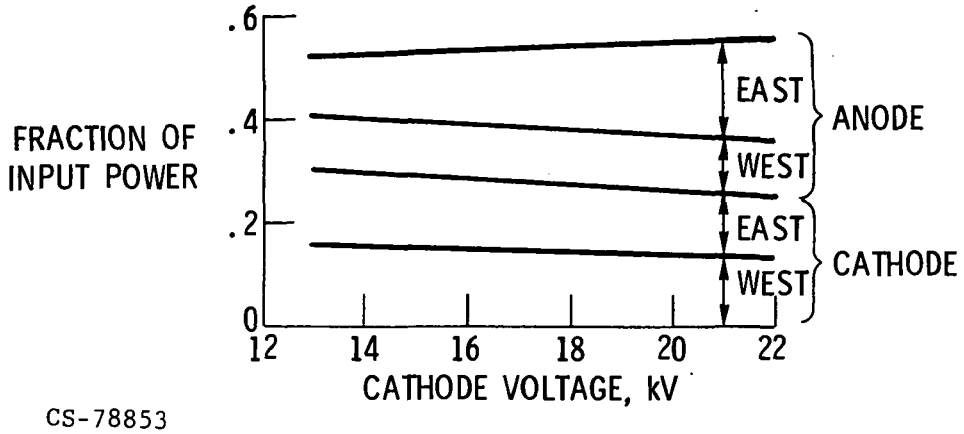

CS-78853

Figure 17. - Electrode power absorption as function of cathode voltage for cathode tips placed outboard from anodes. Cathode tips located at $y = \pm 38$ centimeters; anodes located at $x = 31$ centimeters; anode diameter, 5 centimeters; west gas flow, 0.38 centimeter per second (STP); east gas flow, 0.06 cubic centimeter per second (STP); midplane pressure, 1.7×10^{-2} newton per square meter (1.3×10^{-4} torr).

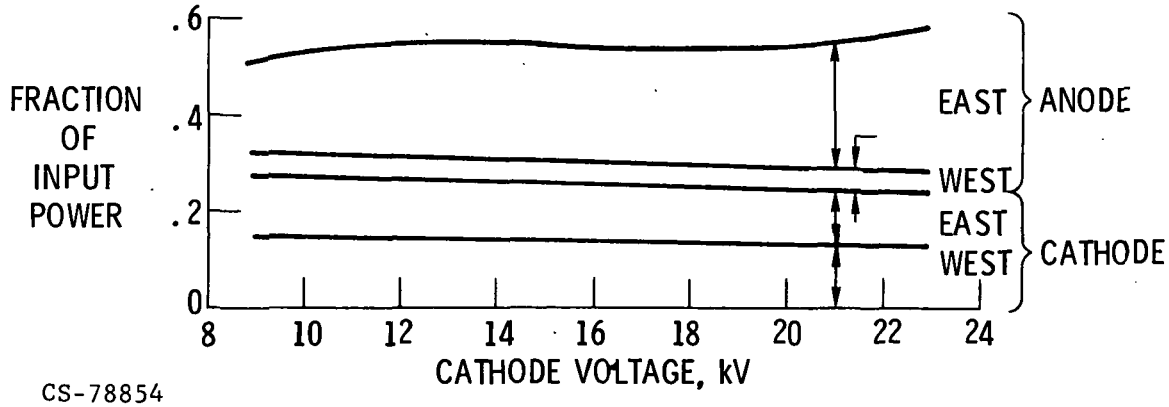

CS-78854

Figure 18. - Electrode power absorption as function of cathode voltage for cathode tips flush with inboard face of anodes. Cathode tips located at $y = \pm 31$ centimeters; anodes located at $x = \pm 31$ centimeters; anode diameter, 5 centimeters; west gas flow, 0.17 cubic centimeter per second (STP); east gas flow, 0.15 cubic centimeter per second (STP); midplane pressure, 1.2×10^{-2} newton per square meter (9×10^{-5} torr).

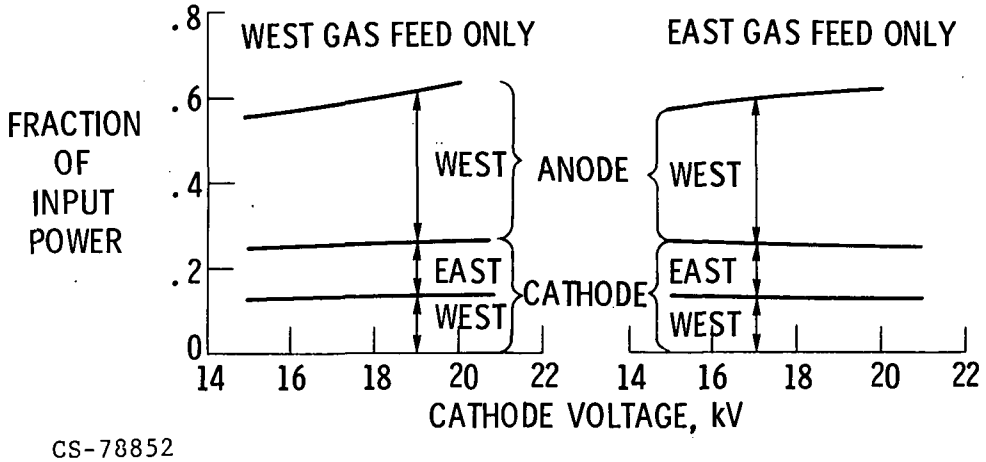

CS-78852

Figure 19. - Electrode power absorption as function of cathode voltage for single-anode operation. Cathode tips located at $y = \pm 31$ centimeters; anode located at $x = -31$ centimeters; anode diameter, 5 centimeters; midplane pressure, 1.1×10^{-2} newton per square meter (8.5×10^{-5} torr); gas flow for west gas feed only, 0.31 cubic centimeter per second (STP); gas for for east gas feed only, 0.31 cubic centimeter per second (STP).

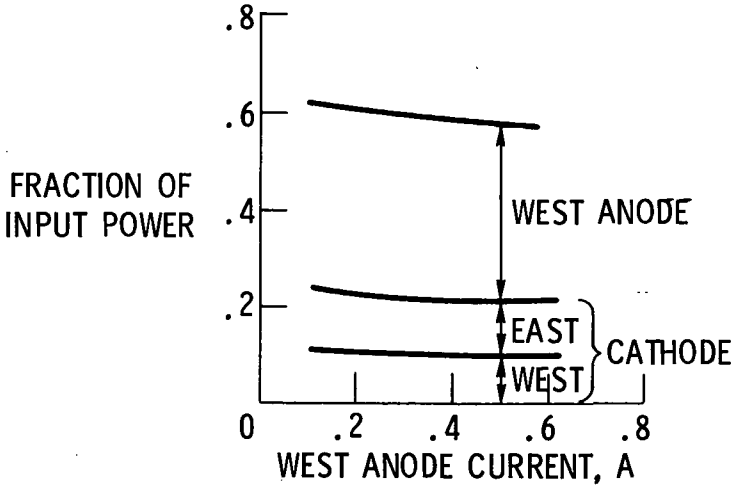

Figure 20. - Electrode power absorption as function of anode current for single-anode operation. Cathode tips located at $y = \pm 31$ centimeters; anode located at $x = -31$ centimeters; anode diameter, 5 centimeters; cathode voltage, 19.9 kilovolts.

NATIONAL AERONAUTICS AND SPACE ADMINISTRATION
WASHINGTON, D.C. 20546

OFFICIAL BUSINESS
PENALTY FOR PRIVATE USE $300

SPECIAL FOURTH-CLASS RATE BOOK

POSTAGE AND FEES PAID
NATIONAL AERONAUTICS AND SPACE ADMINISTRATION
451

U.S.MAIL

POSTMASTER: If Undeliverable (Section 158 Postal Manual) Do Not Return

"The aeronautical and space activities of the United States shall be conducted so as to contribute . . . to the expansion of human knowledge of phenomena in the atmosphere and space. The Administration shall provide for the widest practicable and appropriate dissemination of information concerning its activities and the results thereof."

—NATIONAL AERONAUTICS AND SPACE ACT OF 1958

NASA SCIENTIFIC AND TECHNICAL PUBLICATIONS

TECHNICAL REPORTS: Scientific and technical information considered important, complete, and a lasting contribution to existing knowledge.

TECHNICAL NOTES: Information less broad in scope but nevertheless of importance as a contribution to existing knowledge.

TECHNICAL MEMORANDUMS: Information receiving limited distribution because of preliminary data, security classification, or other reasons. Also includes conference proceedings with either limited or unlimited distribution.

CONTRACTOR REPORTS: Scientific and technical information generated under a NASA contract or grant and considered an important contribution to existing knowledge.

TECHNICAL TRANSLATIONS: Information published in a foreign language considered to merit NASA distribution in English.

SPECIAL PUBLICATIONS: Information derived from or of value to NASA activities. Publications include final reports of major projects, monographs, data compilations, handbooks, sourcebooks, and special bibliographies.

TECHNOLOGY UTILIZATION PUBLICATIONS: Information on technology used by NASA that may be of particular interest in commercial and other non-aerospace applications. Publications include Tech Briefs, Technology Utilization Reports and Technology Surveys.

Details on the availability of these publications may be obtained from:

SCIENTIFIC AND TECHNICAL INFORMATION OFFICE

NATIONAL AERONAUTICS AND SPACE ADMINISTRATION

Washington, D.C. 20546